

**B. TECH. PROJECT
REPORT**

On

**AN EXPERIMENTAL AND
NUMERICAL STUDY OF MULTI-
FIBER MULTI-LAYER GFRP
COMPOSITES**

BY
Bomminayuni manoj-160003013
Narne vamsi-160003033



**DISCIPLINE OF MECHANICAL ENGINEERING
INDIAN INSTITUTE OF TECHNOLOGY INDORE**

Nov 2019

AN EXPERIMENTAL AND NUMERICAL STUDY OF MULTI-FIBER MULTI- LAYER GFRP COMPOSITES

A PROJECT REPORT

*Submitted in partial fulfillment of the
Requirements for the award of the degrees*

Of
BACHELOR OF TECHNOLOGY
In

MECHANICAL ENGINEERING

Submitted by:
Bomminayuni manoj-160003013
Narne vamsi-160003033

Guided by:
Dr. Subbareddy Daggumati
(Assistant Professor)
The discipline of Mechanical Engineering



INDIAN INSTITUTE OF TECHNOLOGY INDORE
Nov 2019

CANDIDATE'S DECLARATION

We hereby declare that the project entitled “**An Experimental and numerical study of multi-fiber multi-layer GFRP composites**” submitted in partial fulfillment for the award of the degree of Bachelor of Technology in ‘**Mechanical engineering**’ completed under the supervision of **Dr. Subbareddy Daggumati, Assistant Professor in Mechanical engineering, IIT Indore** is an authentic work.

Further, I/we declare that I/we have not submitted this work for the award of any other degree elsewhere.

Bomminayuni manoj

Narne vamsi

CERTIFICATE by BTP Guide(s)

It is certified that the above statement made by the students is correct to the best of my/our knowledge.

Dr.Subbareddy Daggumati
Assistant Professor, Discipline of Mechanical Engineering
IIT Indore

Acknowledgments

We wish to thank Dr. Subbareddy Daggumati for his kind support and valuable guidance. We would like to extend our sincere gratitude to him for his willingness to give us valuable advice and direction whenever we approached him with a problem. We are highly indebted to him for his constant support and supervision as well as providing necessary information to complete this project.

We would also like to thank Mr. Akash Sharma (Ph.D. Scholar) for his help.

Without their support, this project would not have been possible.

Bomminayuni Manoj (160003013)

Narne Vamsi (160003033)

B.Tech. IV Year

The discipline of <Mechanical Engineering>

IIT Indore

Abstract

The current study presents a micromechanical Finite Element Analysis (FEA) of Multi-fiber Multi-Layer (M^2RVE) Glass fiber reinforced polymer (GFRP) composites. In order to predict the failure behavior of a composite ply under various load conditions, an RVE (Representative volume element) based approach was used. The selected material is a Non-crimp fabric (GFRP composite), which has both axial and backing fiber bundles oriented perpendicular to each other. To capture the constituent material yield and failure behavior, an M^2RVE model is created with a discrete representation of the various constituent materials such as fiber, interface, interphase, and matrix material. In order to avoid the edge stress concentrations, Periodic Boundary Conditions (PBC's) are applied to surfaces, edges, and vertices of the M^2RVE . The predicted stress-strain behavior under individual load cases is compared to the experimental damage profiles as well as the stress-strain curves. The stress-strain response predicted by the M^2RVE model is in good agreement with the experimental data available. Numerical Failure envelopes for both single RVE and M^2RVE fiber-matrix composites were generated. Furthermore, the effect of backing fiber volume fraction on the M^2RVE stress-strain response under Transverse Tension is investigated. Manufactured epoxy specimens are subjected to the experimental testing under the Tensile load condition to get the stress-strain response of the matrix material. GFRP composites are used in a wide range of applications that deal with different temperature conditions. Hence, the influence of temperature on the M^2RVE stress-strain behavior under Transverse Tension and Transverse Compression is studied.

TABLE OF CONTENTS

ACKNOWLEDGMENTS.....	
SUMMARY	

CHAPTER 1

1.1. Introduction.....	(13-14)
1.2. Fiber Reinforced plastic composite.....	(14)
1.2.1. Non-crimp fabric.....	(14-15)
1.3. State of the art.....	(15-16)
1.4. Goals of the BTP.....	(17)
1.5. Modeling of M ² RVE (<i>Multi-fiber Multi-layer Representative volume element</i>)	
1.5.1 Why M ² RVE?	(17-18)
1.5.2. Constituents of an M ² RVE	(18)
1.6. Boundary Conditions.....	(19)
1.6.1. Implementation of Periodic Boundary Conditions (PBC's).....	(19-20)
1.7. Material Properties.....	(21)

CHAPTER 2

Damage modeling of materials

2.1. Material model and failure criterion.....	(23)
2.1.1. Drucker-Prager plasticity model.....	(23-24)
2.1.2. Damage modeling of Interface and backing fibers.....	(24-26)

CHAPTER 3

Results and Discussion

3.1. M ² RVE under Transverse Tension.....	(28-29)
3.2. M ² RVE under Transverse Compression.....	(29-31)
3.3. M ² RVE under In-plane Shear.....	(31-33)
3.4. Failure Envelope in 0-90 ⁰	(33)
3.5. Effect of backing fiber volume fraction on M ² RVE.....	(34-35)
3.6. Conclusion.....	(35)

CHAPTER 4

Environmental effects on M²RVE and experimental testing of epoxy under transverse tension

4.1. Influence of Temperature on M ² RVE under Transverse Tension.....	(37-38)
4.2. Influence of Temperature on M ² RVE under Transverse compression....	(38-39)

4.3. Failure behavior of an epoxy resin under Transverse tension..... (40-41)
 4.3.1 Introduction..... (40)
 4.3.2 Material and mechanical tests..... (40)
 4.3.3 Results and discussion..... (41)
 4.3.4 Conclusions..... (41)

References.....(42-43)

List of figures

Figure 1.1: Fiber architecture of non-crimp fabric in Axial Face and Backing Face.....	(15)
Figure 1.2: NCF Fiber architecture	(15)
Figure 2: Constituents of the fiber-matrix boundary region	(18)
Figure 3: Different Constituents in the Model of M^2RVE	(19)
Figure 4: Simulated Load conditions.....	(19)
Figure 5.1: Periodic array of 3D RVE.....	(20)
Figure 5.2: Application of Periodic Boundary Conditions on 3D RVE	(20)
Figure 6.1: Von-mises and drucker prager yield surfaces.....	(23)
Figure 6.2: Linear Drucker-Prager model.....	(23)
Figure 7.1: Interface between fiber and matrix.....	(25)
Figure 7.2: Interface layer in between fibers.....	(25)
Figure 7.3: Different modes of Failure.....	(25)
Figure 7.4: Traction Separation graphs for independent single.....	(26)
Figure 8.1: Stress contour under transverse tension.....	(28)
Figure 8.2: Crack in Interface Elements.....	(28)
Figure 9: Crack in the Backing fibers	(28)
Figure 10: Experimental vs numerical Stress-Strain curve under Transverse Tension.....	(29)
Figure 11: Stress contour under Transverse Compression	(30)
Figure 11.2: Plastic Strain contour under Transverse Compression.....	(30)
Figure 12: Experimental vs numerical Stress-Strain curve under Transverse Compression...	(31)
Figure 13.1: Stress contour under In-Plane Shear Loading.....	(32)
Figure 13.2: Interfacial debonding along the ultimate failure surface.....	(32)

Figure 14: Experimental vs Numerical Stress-Strain curve under In-plane Shear.....(33)

Figure 15: failure envelope of RVE and M²RVE.....(33)

Figure 16 : Experimental vs numerical Stress-Strain curve under Transverse Tension for different
Volume fractions.....(34)

Figure 17: Stress strain response of epoxy 1135i at different temperatures under transverse
tension..... (37)

Figure 18: Stress strain response of M²RVE at different temperatures under transverse tension..(38)

Figure 19: Stress strain response of epoxy E832 at different temperatures under transverse
Compression.(39)

Figure 20: Stress strain response of M²RVE at different temperatures under transverse compression

Figure 21: Tensile specimen[ASTM D638](39)

Figure 22: Stress-strain response of epoxy under transverse tension(40)

Figure 23: Specimen after failure.....(41)

List of tables

Table 1: Property Table of M²RVE.....(21)

Table 2: Effect of backing fiber volume fraction on M²RVE.....(35)

CHAPTER 1

1.1. INTRODUCTION:

A Composite is a material made from two or more constituent materials with different physical or chemical properties, that, when combined produce a material with characteristics different from individual constituents. Composite materials are widely used in buildings, bridges, and structures such as boats, airplanes, racing car bodies, etc. They are becoming increasingly popular in aerospace and other industries due to their high strength to weight ratio. As a result of these widespread applications of composite materials, the need for a better understanding of them has emerged. The fiber-reinforced polymer also known as Fiber-reinforced plastic (FRP) is a composite material made of a polymer matrix reinforced with fibers. Commercial material commonly has glass or carbon fibers in matrices based on thermosetting polymers, such as epoxy or polyester resins. A Glass fiber reinforced plastic (GFRP) composite also known as fiberglass is one of the most widely used fiber-reinforced material and is in high demand for its High strength, low-cost, lightweight and corrosion resistance quality. Glass fibers when coupled with various plastics, it possesses a chemical inertness which renders the composite to be used in a variety of environments. These attributes of GFRP composites contribute to its use in a broad range of applications in industries such as wind energy, aerospace, and defense, construction, automotive, marine, etc. As a fiber Glass is relatively strong, and when embedded in a plastic matrix, it produces a composite structure of very high strength.

GFRP composites are frequently used in wind-turbine blade design. The general requirements for material selection of a wind turbine rotor blades are high stiffness, low density, and long fatigue life. Glass fiber reinforced composite fits these requirements. In this Perspective, an attempt has been made to study these composites by performing Finite Element Analysis (FEA) based on micro-mechanics theory. The microstructure of these composite materials depicts randomly oriented fibers within the matrix. Hence, FEA is performed on an RVE Model chosen from the composite Laminate. An RVE (Representative volume element) is the smallest volume over which a measurement can be made that will yield a value representative of the whole.

Although experimental testing can be performed on GFRP composite specimens, results obtained from such testing processes usually yield a limited range of details about the composite. Therefore,

simulations are performed to validate the experimental results. In addition, damage initiation sites under static loading may be approximated by the properties of each constituent material. Furthermore, Constituent stress-strain behavior, as well as the damage progression in the composite, can be predicted by performing micro-mechanical simulations.

In this study, a three-dimensional Multi-Fiber Multi-Layer micromechanical model is developed to predict the mechanical behavior and study the effect of various parameters on the damage response of the Composite. Different failure mechanisms such as fiber fracture, matrix plastic damage and fiber-matrix interface debonding may take place based on the subjected load conditions. Hence, the chosen RVE model is simulated for different load conditions in order to capture the material yield and failure behavior as well as the stress-strain responses of the composite.

1.1.1 Motivation

The main motivation is to identify when damage will occur or the onset of damage occurs when using these composite materials. These composite materials are used in the design of many sophisticated structures such as in wind turbine blades, construction & infrastructure, Aerospace, and Defense, etc.

For a better material design using these composite materials, skills within all the characteristic length scales such as structural, component, Laminate scale, etc are necessary. However, the focus area of this study is the microscale level since damage within the composite structures always initiates at the micro-scale level and progresses till final failure. The outcome of this study would be a damage-resistant composite design by an understanding of the effects of individual constituents on the damage behavior of the composite until the final failure.

1.2. Fiber Reinforced plastic composite:

1.2.1 Non-crimp Fabric

Non-crimp fabrics (NCF's) are used commonly in the material selection of wind turbine blades. Hence, the type of material used in our study is a Non-crimp fabric. Non-crimp fabrics (NCFs) differ from woven fabrics by a stitching material (polyester yarn) that is introduced to bind several

unidirectional fiber layers to avoid misalignments. Fiber-reinforced composite such as NCF (Non-crimp Fabric) typically consists of fiber bundles stitched together to form a fabric as shown in fig 1.1

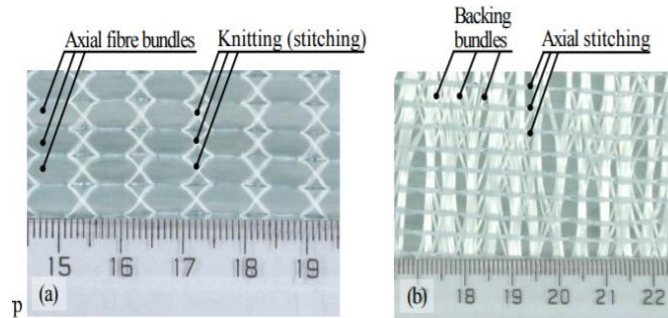


Fig 1.1: Fiber architecture of NCF (a) Axial Face (b) Backing Face [1]

In these NCF's while the primary reinforcing strands (axial fibers) are placed in the longitudinal direction, the fabric also consists of transverse backing glass strands (Lower Volume Fraction) to which the primary strands are stitched. Despite the wide range of applications of NCF's, very limited information is available on the mechanical performance of these composites. Hence, a multi-fiber multi-layer RVE model representing longitudinal axial fibers in the top RVE and transverse backing fibers in the bottom RVE has been developed to predict the failure mechanisms and stress-strain responses for different load conditions. Furthermore, the FEA model is developed using the microscale image of the material which captures the fiber architecture.

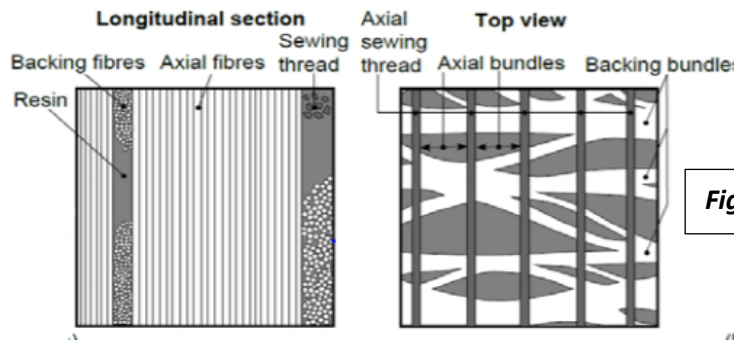


Fig1.2: NCF Fiber architecture [5]

1.3. State of the Art:

At present, the study of GFRP composites is limited to a single RVE based model with only the axial fibers taken into account [7]. Most of the RVE Models typically use a single fiber to predict the properties of the composite which is not a very accurate representation [4]. A few studies which

have been reported on the prediction of micro-damage via a multi-fiber RVE model does not consider the effect of finite thickness interphase [2]. The multi-fiber multi-Layer RVE approach was used to predict the in-plane shear response of the Composite [5][6] but finite interphase thickness was not implemented. Despite the wide range of applications of Non-crimp Fabric(NCF), very limited information is available on the mechanical performance of these composites. In order to incorporate all the constituent materials of an NCF (Non-crimp fabric) into our FE model, a Multi-fiber Multi-layer(M²RVE) model is developed to capture the material yield and failure behavior. While Axial fibers are placed along the longitudinal direction, backing fibers are placed along the transverse direction perpendicular to axial fiber bundles.

Based on a Literature Review, it can be inferred that a micromechanical M²RVE model consisting of both Axial and backing fibers has not been implemented yet. Hence a multi-fiber multi-layer (M²RVE) has been modeled using ABAQUS Software. The strength and damage resistance of composites can be predicted and ultimately improved if the effects of individual constituents such as fiber, matrix, and interface on the composite yield and failure behavior are better understood.

[2] reported Fatigue damage propagation in unidirectional glass fiber reinforced composites made of a non-crimp fabric. It was observed that the transverse crack in a non-crimp fabric propagates along the arc of axial fibers in a nearly straight line through the entire layer thickness. Subsequently, Crack in the axial fibers is then propagated as fiber debonding in backing fibers. Hence, the main goal of this study is to understand damage initiation and propagation until the final failure when subjected to static load conditions.

1.4 Goals:

Considering the above shortcomings, the following goals are set.

- To perform microscale damage analysis on M²RVE GFRP composites subjected to different types of loading.
- Simulating the fiber fracture along with the 90-degree ply microscale damage and plotting the stress-strain curve under tensile load
- Generating the RVE & M²RVE failure envelopes for GFRP composite.
- Effect of backing fiber volume fraction on Stress-Strain response of the composite under transverse Tension.

- Influence of Temperature on M^2RVE under Transverse Tension and Transverse Compression.
- Experimental Testing of Epoxy specimen under Tensile load.

The most important goal of this study is to identify when damage will occur. To do so, the M^2RVE model developed is subjected to different load conditions (Transverse tension, Transverse Compression, In-plane shear)

1.5. Modeling of M^2RVE :

1.5.1. Why M^2RVE ?

An RVE (Representative volume element) is the smallest volume over which a measurement can be made that can be representative of the whole. A multi-fiber multi-layer RVE consists of two RVE's with one placed on top of the other. The type of material used in our study is a non-crimp fabric. As discussed above, a non-crimp fabric has two fiber bundles (axial & backing) oriented perpendicular to each other. A single RVE model hinders the possibility to incorporate perpendicularly oriented fiber bundles. Hence a multi RVE model is necessary to incorporate both axial fibers as well as backing fibers into our FE model.

An M^2RVE model is generated with a random distribution of axial and backing fibers. The overall volume fraction of these randomly distributed fibers is about 52 percent [1] in which axial fibers constitute 49 percent and backing fibers make up 3 percent. Axial fibers and backing fibers have a diameter of about $17\mu\text{m}$ and $9\mu\text{m}$ respectively [1].

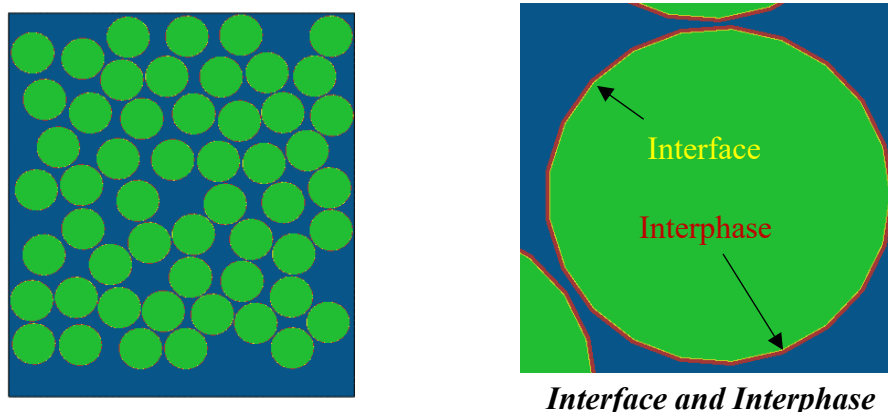


Figure 2: Constituents of the fiber matrix boundary region

The fiber-matrix boundary is made up of interface elements and the interphase region as shown in figure 2. The interface region exhibits cohesive behavior whereas the Interphase region acts as an intermediate phase between two materials in equilibrium. The M^2RVE model was meshed using C3D8R Elements. Cohesive elements (COH3D8) were used to represent the interface region. M^2RVE model developed is shown in the below figure 3. The FE mesh consists of a total of 76449 nodes.

This proposed M^2RVE model is subjected to Transverse Tension, Transverse Compression and In-Plane Shear loading using periodic boundary conditions. The stress-strain curves obtained from these simulations for different load conditions are then compared with the experimental stress-strain curves. The dimensions of the RVE are 137.51 μm (length), 159.51 μm (height), 25 μm (depth). Cohesive elements are easily damageable elements which exhibit cohesive behavior.

1.5.2. Constituents of an M^2RVE :

Different constituents of an M^2RVE model are shown in fig 3. Axial fibers are placed along the longitudinal direction(z-direction), whereas backing fibers are placed along the transverse direction(x-direction). Interface elements and interphase regions have a thickness of about 50nm and 200nm respectively.

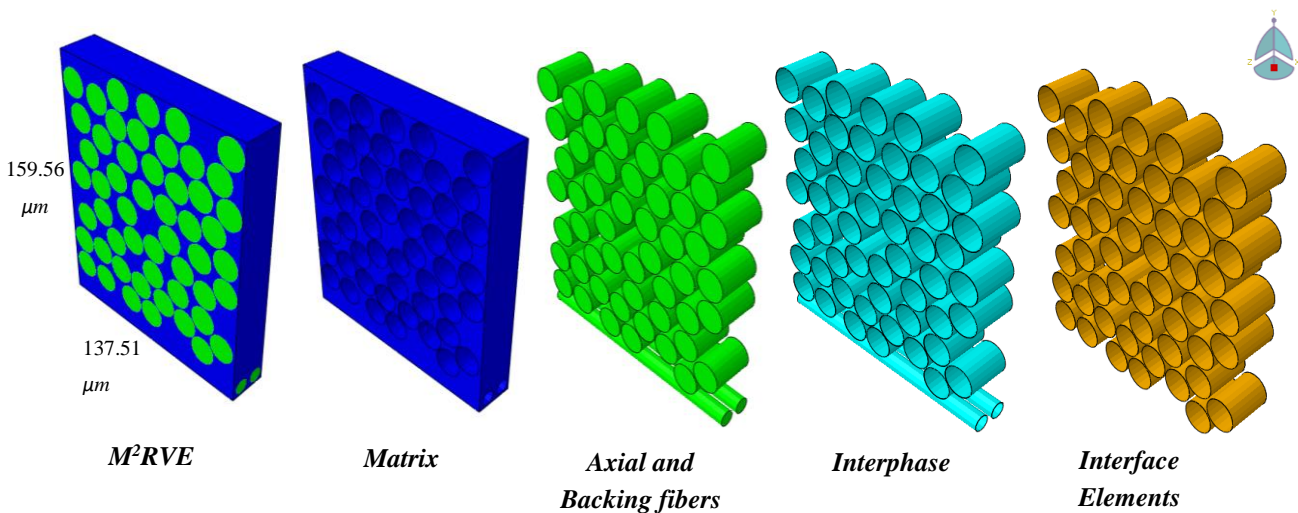


Fig 3: Different Constituents in the Model

1.6. Boundary Conditions:

This M²RVE model is subjected to Transverse Tension, Transverse Compression, and IN-Plane Shear loading as shown in figure 4 and their corresponding results are presented in this report.

Periodic boundary conditions are used to implement these load conditions into our FE model.

Here the backing fibers placed linearly along the x-direction are under longitudinal loading when M²RVE is subjected to Transverse Tension/ Compression.

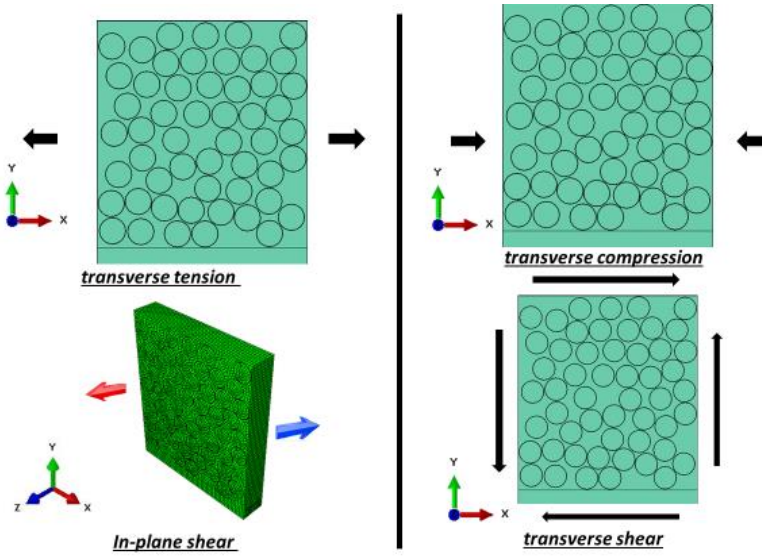


Figure 4: Simulate Load conditions

1.6.1. Implementation of Periodic Boundary Conditions (PBC's)

Periodic Boundary Conditions(PBC) are applied to avoid non-linear stress-strain states. The PBC makes it possible to represent an infinitely large system using a small domain replicated in the three spatial directions.

PBC's are formulated in 3D assuming a cuboid unit cell as shown in figure 5. The relative displacement between nodes located on a pair of opposite surfaces is given by

$$u_i^{k+} - u_i^{k-} = \overline{S}_{ij}(x_i^{k+} - x_i^{k-})$$

where, S_{ij} is the macro-strain tensor of the unit cell, and l_i is the length of the unit cell in i direction between opposite surfaces? u_i is the displacement on the face of the RVE. Where 'k+' means

displacement along the positive x_i direction, and 'k-' means displacement along negative x_i direction on the corresponding surfaces M-/M+, N-/N+, and O-/O+(shown in Fig 5.2). For each direction i that links nodes in opposite surfaces, there is a dummy node with three displacement components j .

The dummy nodes are usually introduced as reference points that are not attached to any other part of the model. These reference points make possible to easily set any kind of boundary condition. Then, the model can be reused for different load conditions changing only the displacement of these reference points.

To generate these linear constraint equations MATLAB code has been used for all the nodes on opposing faces. The obtained values of Average Stresses and Strains for every increment are then used to plot the stress-strain response for the given load condition.

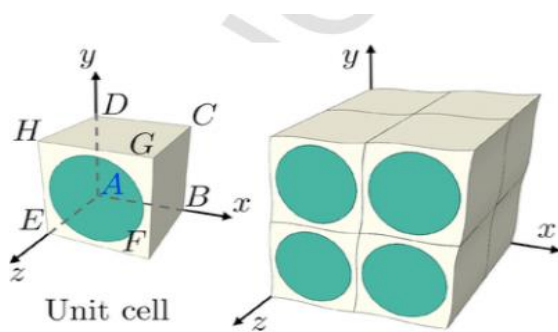


Figure 5.1: Periodic array of 3D RVE [8]

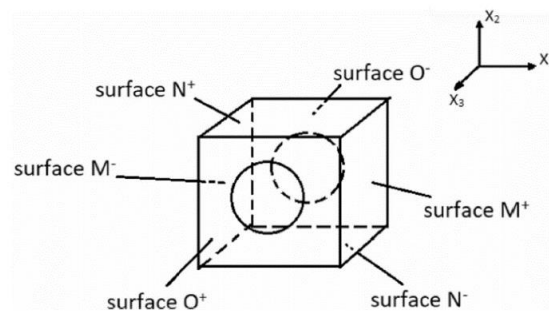


Figure 5.2: Application of Periodic Boundary Conditions on 3D RVE [11]

To generate these linear constraint equations, MATLAB code has been used for all the nodes on opposing faces. The obtained values of Average Stresses and Strains for every increment are then used to plot the stress-strain response for the given load condition.

1.7. Property Table:

A glass fiber reinforced polymer consists of epoxy material as the matrix. Glass fabric/epoxy laminates were composed of Vectorply E-LT-5500 infused with Epikote MGS RIMR 135/Epikure MGS RIMH 1366 (100 to 30 mass ratio) epoxy resin.

The properties of different constituent elements are shown in the following table

Property	Fibers (E- glass)	Matrix (epoxy)	Interface	Interphase
Elastic Modulus(E) (Gpa)	74[13]	3.6[13]	-	1.9[14]
Poisson's Ratio	0.26[13]	0.35[13]	-	0.4[14]
Strength (Mpa)	1649[14]	-	53/120/120[15]	-
Stiffness(N/mm^3)	-	-	1e8[16]	-
Fracture Energy(N/mm)	-	-	[0.01,0.025,0.025]	-
Drucker-Prager Parameters- [β/K]	-	[23.2°/0.875]	-	[23.2°/0.875]

Table1: properties of different constituents

CHAPTER 2

2.1. Material model and failure criterion:

Material plasticity is usually modeled by Tresca or the Von Mises criteria. They do not take hydrostatic pressure into account and are suitable for the modeling of plasticity in metals. However, for materials such as rock, concrete, and polymers, it is not suitable as there is a strong dependence on the **hydrostatic pressure**. Hence, we need a pressure-dependent yield criterion so that it can capture the effect of hydrostatic Stresses.

In addition to the material plasticity, the Fiber-Matrix interface region exhibits cohesive behavior. Damage in this region is governed by Damage initiation and Damage evolution criteria. QUADS criteria is used for Damage initiation and BK-law is used for damage evolution.

2.1.1 Drucker-Prager Criteria:

In order to model the plasticity of epoxy resin (matrix), we have used Drucker-Prager Criteria as it considers the effect of hydrostatic Stresses. It is a simple modification of the Von Mises criterion, and it is represented by the equations

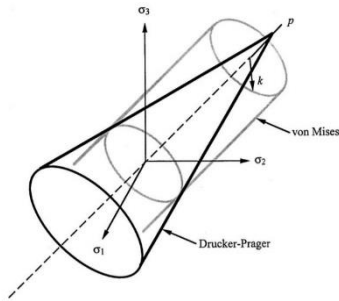


Figure 6.1: Von-mises and Drucker Prager yield surfaces

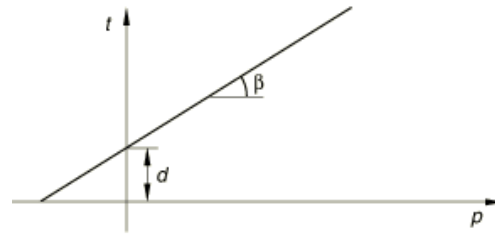


Figure 6.2: Linear Drucker-Prager model [12]

$$F = t - p \tan \beta - d = 0$$

$$t = \frac{1}{2} q \left[\left(1 + \frac{1}{K}\right) - \left(1 - \frac{1}{K}\right) \left(\frac{r}{q}\right)^3 \right], \text{ where}$$

- β is the slope of the linear yield surface in P-t stress plane
- d is the cohesion yield stress
- K = ratio of the yield stress in triaxial tension to that in triaxial compression
- r = third stress invariant of deviatoric stress
- q = Von-Mises stress
- p = hydrostatic stress

The input parameters to implement this criterion in Abaqus are β and K . these are calculated using the relation between the Mohr-Coulomb and the Drucker-Prager yield criteria. This gives us the relation between tensile and compression strengths with the cohesion stress and friction angle as

$$\sigma_{mt} = 2c \frac{\cos \phi}{1 + \sin \phi}; \sigma_{mc} = 2c \frac{\cos \phi}{1 - \sin \phi}$$

The internal friction angle ϕ of the epoxy obtained is 2.5° . the slope of the yield surface (β) for the Drucker-Prager plasticity model is calculated using the following equations

$$\tan \beta = \frac{6 \sin \phi}{3 - \sin \phi}; K = \frac{3 - \sin \phi}{3 + \sin \phi}$$

β and K value obtained are 10.,0.92

2.1.2 Cohesive zone model:

To show fiber fracture and Fiber-Matrix interface damage at the micro-scale level, the response of the cohesive element is used. These interface elements are introduced as a 3-D layer of cohesive elements (COH3D8) between Fiber and Matrix, and for fiber fracture, they are randomly placed along the fibers to create fracture planes.

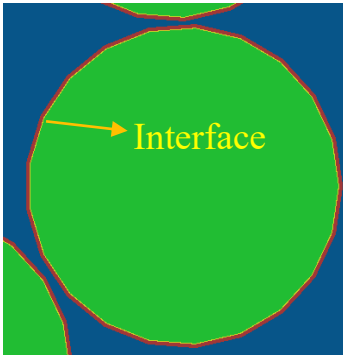


Figure 7.1: Interface between fiber and matrix

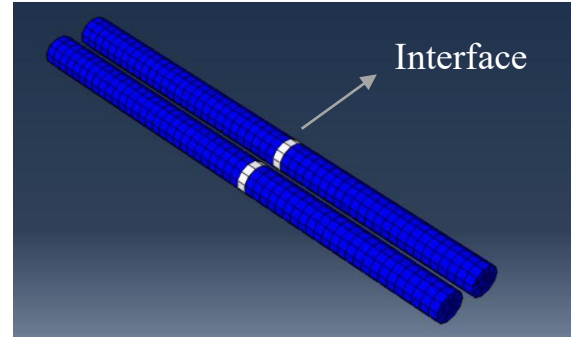


Figure 7.2: Interface layer in between fibers

It is defined by bi-linear traction-separation law, which shows that separation displacement between the top and bottom faces of the element is dependent on the traction vector acting on it. Initially, the response is linear with an elastic stiffness K , and there is no damage seen.

$$T_{n/s} = Kd_{n/s}$$

The quadratic nominal stress criterion is used for **Damage initiation** criterion which is represented by the equation

$$f = \left\{ \frac{\langle t_n \rangle}{t_n^0} \right\}^2 + \left\{ \frac{t_s}{t_s^0} \right\}^2 + \left\{ \frac{t_t}{t_t^0} \right\}^2.$$

Where, T_n^0 , t_s^0 , and t_t^0 are peak values of the nominal stress for single independent modes (shown in fig). Where $\langle \rangle$ is the Macaulay brackets, which return the argument if positive and zero, it means that there is no development of damage when the interface is under compression.

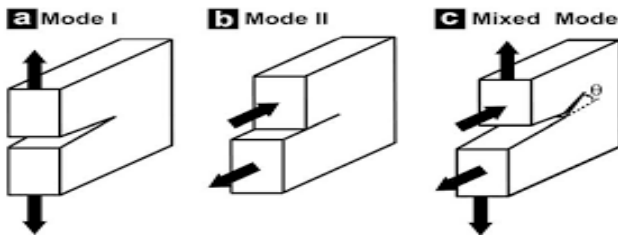


Figure 7.3: Different modes of Failure

BK law is used for the **Damage Evolution** criterion when the damage begins, and the traction stress decreases depending on the interface damage parameter D , which evolves from 0 (absence of damage) to 1 (ultimate failure). The displacement at failure is determined by the fracture energy G , which corresponds to the area under the traction-separation curve and is given by

$$G_{equivC} = G_{IC} + (G_{IIC} - G_{IC}) \left(\frac{G_{II} + G_{III}}{G_I + G_{II} + G_{III}} \right)^\eta.$$

$G_S = G_s + G_t, G_T = G_n + G_s; \eta = \text{Mixed mode interaction parameter}$

$G_n^c/GIc, G_s^c/GIIC$ and $G_t^c/GIIIC$ are critical fracture energies required to cause failure in the single independent modes (shown in fig).

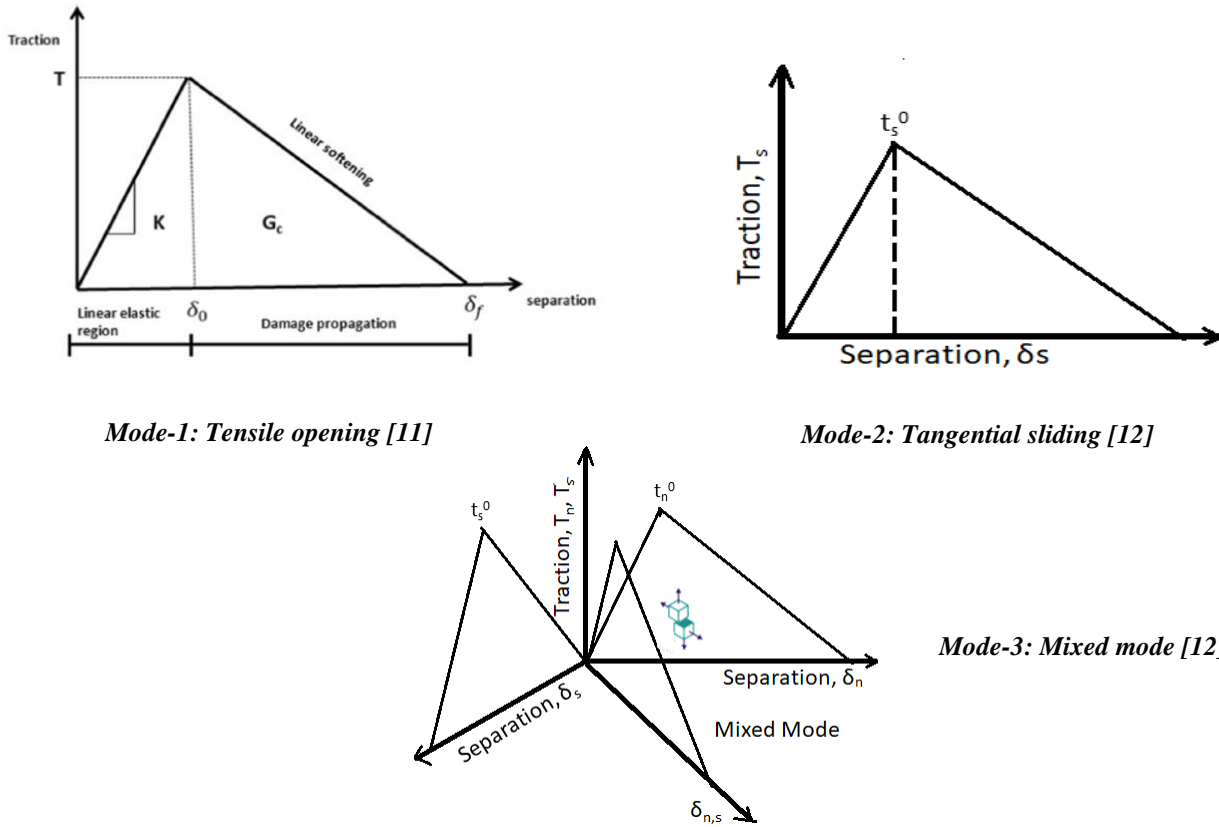


Figure 7.4: Traction Separation graphs for independent single

CHAPTER 3

Results and Discussion

3.1 M²RVE under Transverse Tension:

When the proposed M2RVE model is subjected to transverse tension(5 % strain), it can be observed that the damage initiates in the form of interfacial debonding, which first grows along the arc direction of the fiber. At a certain critical size, they kink out of the interface and lead to the onset of matrix micro-crack.

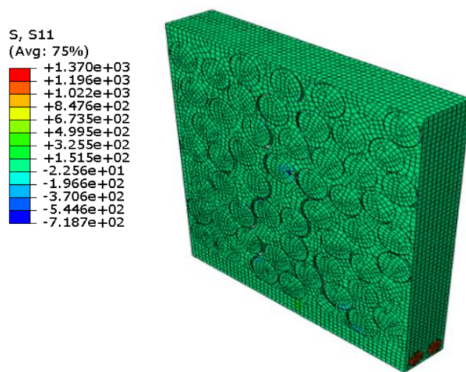


Figure 8.1: Stress contour under transverse tension

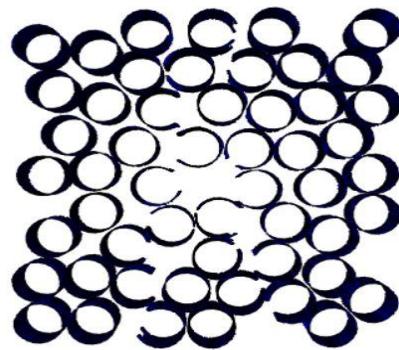


Figure 8.2: Crack in Interface Elements

The stress-strain response shown in fig 8.1 indicates that the maximum stress values can be observed in the backing fibers due to its high stiffness value. Stress values in backing fibers increase with increasing load.

Further Load increments lead to the cracking of backing fibers (Fig 9) when the critical stress (tensile strength) value of 1649Mpa is achieved.

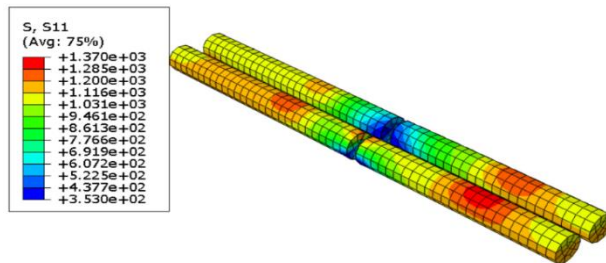


Figure 9: Crack in the Backing fibers

The average Stress-Strain values obtained for each increment are then plotted along with the experimental data [3], as shown in fig 10.

- ❖ Modulus(E) calculated from the FEA Simulation curve is found to be 16 Gpa, whereas the experimental data suggest a value of 17.2 Gpa with a Standard deviation of 2 Gpa.
- ❖ The Ultimate Strength value obtained from the numerical simulation is 72.3Mpa compared to an experimental value of 73Gpa. The corresponding average strain value is about 0.52%. Stress values drop significantly after this point as a result of a crack in the backing fibers.

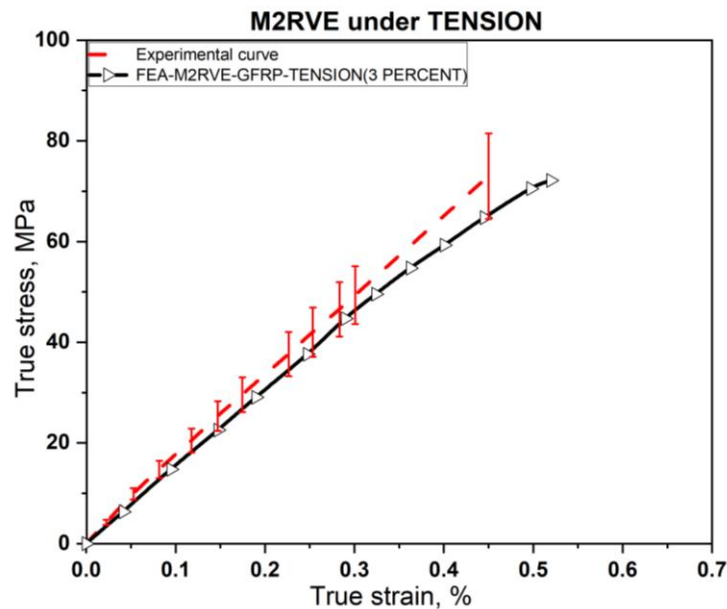


Figure 10: Experimental [3] vs numerical Stress-Strain curve under Transverse Tension

The stress-strain curve under transverse tension can be divided into three regimes. The initial, elastic region where stress increases linearly with strain until the point of damage initiation. With the damage evolution of the constituents, the slope gradually decreases with increasing strain. when strain exceeds 0.52% plastic deformation region is formed during which the stress values drop significantly with increasing strain.

3.2 M²RVE under Transverse compression:

The contour plot of the plastic strains in the matrix showed that failure took place by the propagation of a shear band in the matrix (shown in fig 11.2). The shear band cannot propagate

through the fibers, leading to slight variations in the orientation, which are controlled by the details of the fiber arrangement. The average orientation of the fracture plane was 47.8° , slightly higher than 47.5° , the theoretical value predicted.

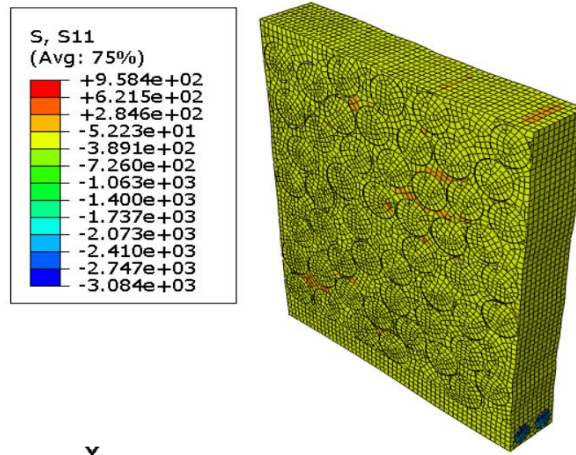


Figure 11.1: Stress contour under Transverse Compression

The analysis has shown that damage initiation in transverse compression took place in the absence of interface decohesion by the nucleation and propagation of a set of plastic shear bands in the matrix. Then Interface cracks promoted the localization of damage in one single shear band, whose precise orientation depended on the details of the fiber spatial distribution, that did not always grow along the theoretical angle.

Further load increments lead to the kinking of backing fibers. The maximum stress values can be seen in the backing fibers due to its high stiffness value in the load direction. The average Stress-

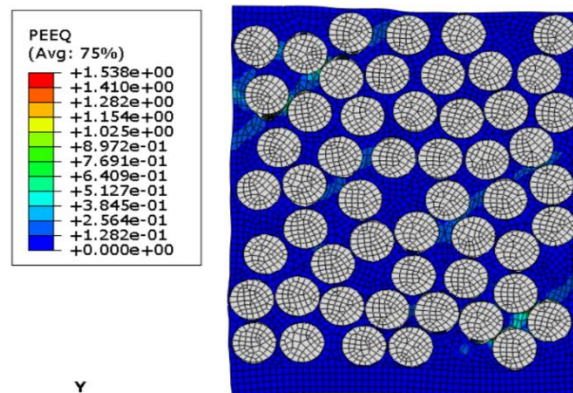


Figure 11.2: Plastic Strain contour

Strain values obtained for each increment are then plotted along with the experimental data [3], as shown in fig 12.

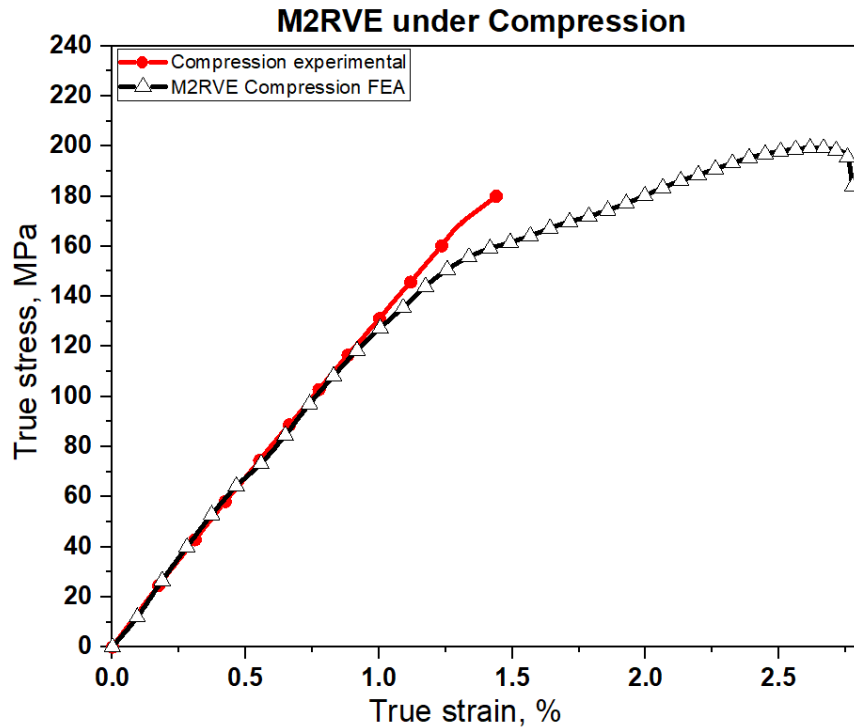


Figure 12: Experimental [3] vs numerical Stress-Strain curve under Transverse Compression

- ❖ Modulus(E) calculated from the FEA Simulation curve is found to be 13.7 Gpa, whereas the experimental data suggest a value of 13.8 Gpa with a Standard deviation of 0.79 Gpa.
- ❖ The ultimate Strength value obtained through numerical simulation is 196Mpa, whereas the experimental data suggest a value of 189 Mpa with a standard deviation of 7.2 Mpa

3.3 M²RVE under In-Plane Shear :

When M²RVE is subjected to In-Plane Shear Loading, it can be observed that the RVE is broken up along the ultimate failure surface. Damage initiates in the form of interfacial debonding near the front and Rear surfaces, and the intermediate part of the fracture surface consists of matrix damage that connects the front and rear interfacial debonding by stair-step pattern. Thus, when the M²RVE model is subjected to in-plane shear, damage first occurs in the form of interfacial debonding near the outer surface; then matrix plastic damage is induced at the vicinity of the interface damage and gradually propagates inward; finally, the matrix damages are linked as a complete surface across the fiber direction, causing the ultimate fracture of the composite.

The average Stress-Strain values obtained for each increment are then plotted along with the experimental data [], as shown in fig 13.

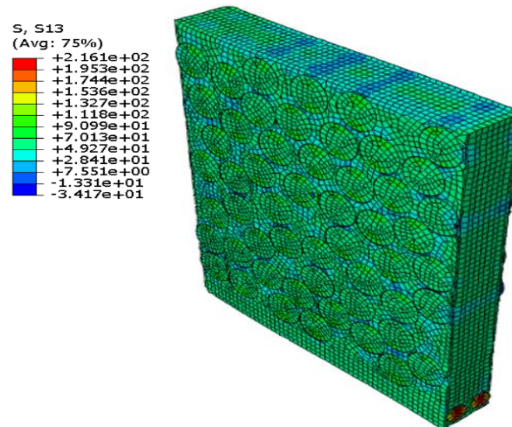


Figure 13.1: Stress contour under In-Plane Shear Loading

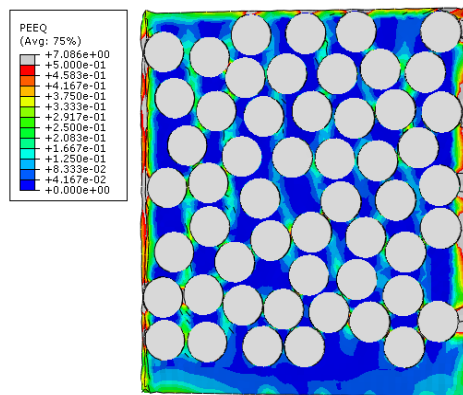


Figure 13.2: Interfacial debonding along the ultimate failure surface

The results show that the interface de-cohesion limits the load transfer from the matrix to the fibers under in-plane shear loading leading to a reduction in the slope of the linear hardening region after matrix yielding. The ultimate shear strength value obtained is 57.64Mpa

The Stress-strain curve under In-plane shear can be divided into two regimes. The initial, elastic region during which stress increases linearly with strain. It is followed by a non- linear region which begins with the onset of matrix plastic deformation until it reaches a peak value (ultimate strength) of 57.64Mpa

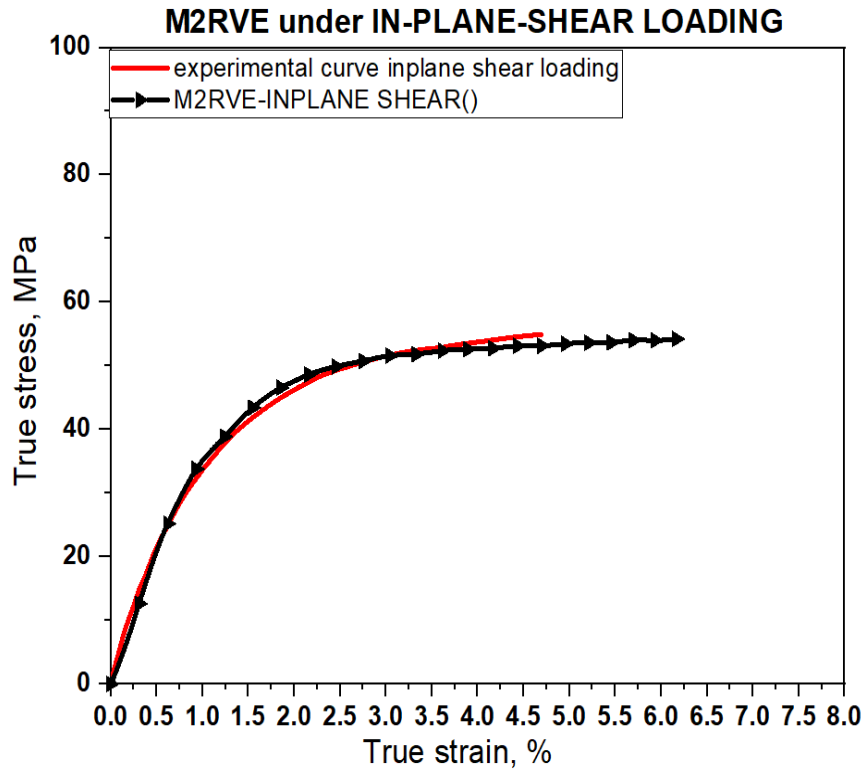
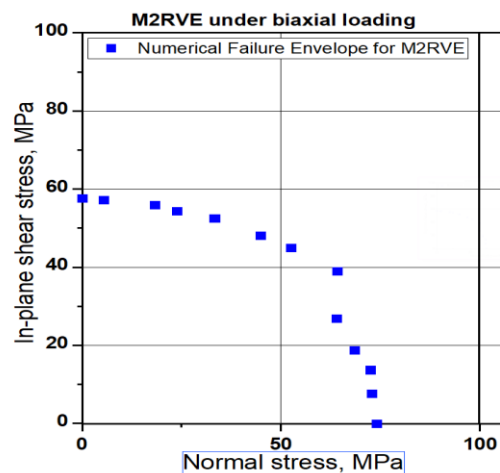
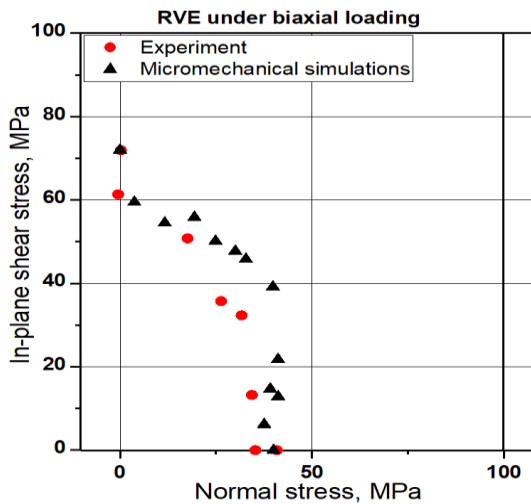


Figure 14: Experimental [3] vs Numerical Stress-Strain curve under In-plane Shear

3.4 Bi-Axial Failure Envelope:

A Failure Envelope is the locus of all the failure Normal and Shear stresses at failure. Taking 0° as transverse tension and 90° as in-plane shear, a graph is plotted between normal stress and in-plane shear stress as a failure envelope from $(0-90)^\circ$ for both single-layer RVE and M^2RVE . We can observe the difference between them as the normal stresses in M^2RVE increased by 80% to RVE. This is due to the 3% backing fiber volume fraction.



3.5 Effect of backing fiber volume fraction on M²RVE:

As we have observed that the strength of M²RVE under transverse tension increased predominantly when compared to the RVE. For a better understanding of this, a parametric study has been done. Keeping the total volume fraction of the M²RVE constant (55%), we have changed the backing fiber volume fraction from (2 - 10) %, As expected, with the increase in the backing fiber volume fraction, both tensile strength and modulus increases predominantly. This can be attributed to the fact that when M²RVE is subjected to Transverse Tension, the backing fibers are under longitudinal loading. As the fibers have very high stiffness in this direction, there is an increase in induced stresses in the backing fiber region which leads to the rise in average values of stresses.

There is no effect of backing fiber volume fraction on the In-plane shear stress-strain response. This is also evident during the comparison of the failure envelope between RVE and M²RVE in the previous section. The in-plane shear strength remained constant at 60 Mpa despite the 3% increase in backing fiber volume fraction.

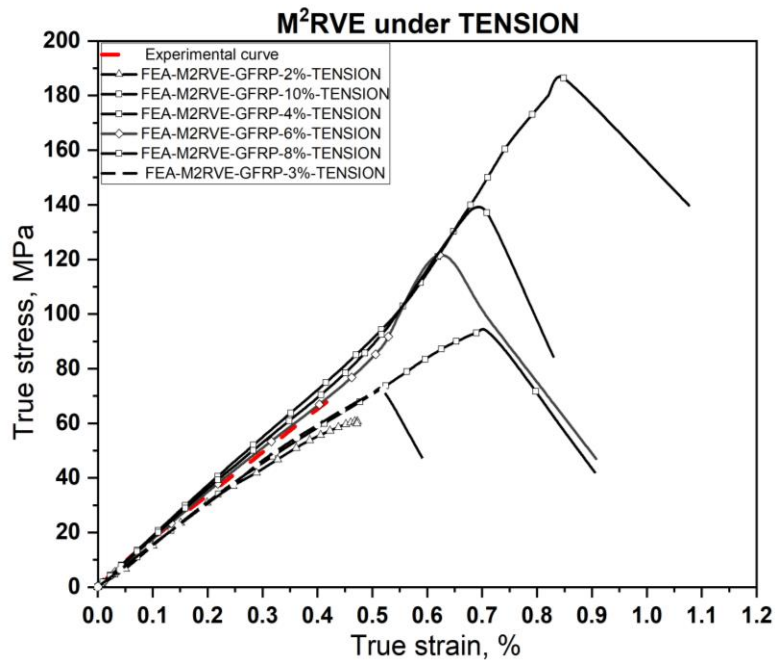


Fig.16. Experimental [15] vs numerical Stress-Strain curve under Transverse Tension for different Volume fractions

Backing fiber volume fraction	Modulus of Elasticity (Gpa)	Tensile strength (Mpa)
2%	1.446	60.6
3%	1.556	72.3
4%	1.604	95.1
6%	1.920	120.9
8%	2.011	137.1
10%	2.2	186.9

Table2: effect of backing fiber volume fraction on M²RVE

3.6 Conclusions:

- Mode-1 (tensile opening) properties predominantly influence interface cracking in transverse tension.
- The In-plane Shear failure of the composite is initiated by interfacial debonding and then dominated by matrix plastic damage.
- When M²RVE is subjected to Transverse Compression a network of shear bands in the matrix are propagated at an angle of 47.8°.
- Numerical results obtained through current methodology are consistent with the experimental results both qualitatively and quantitatively.

CHAPTER 4

4.1 Influence of Temperature on M²RVE under Transverse Tension:

GFRP composites are used in a wide range of applications that require sustaining different environmental conditions. They are used in hot conditions of Aircraft applications as well as cold conditions of offshore wind turbines. We know that epoxy material is sensitive to temperature changes and hence the properties of the material change with temperature. The experimental data of Epoxy L135i(as shown in fig.17) at different temperatures are used to provide the matrix material property data needed for analysis of M²RVE at different Temperatures. The experimental data provides the stress-strain behavior of the matrix from -40⁰ Celsius to 80⁰ Celsius.

The transition temperature of the chosen Epoxy is $(T_g = 90^0 \text{ C})$. As temperature increases the modulus of elasticity decreases and as temperature decreases modulus of elasticity increases.

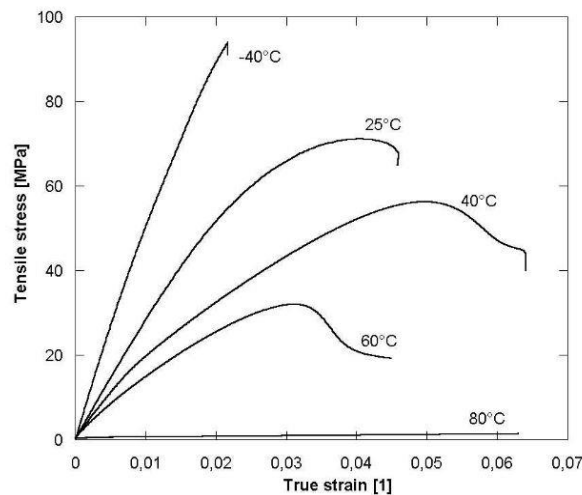


Fig.17. Stress strain response of epoxy l135i at different temperatures under transverse tension [18]

According to DNVGL, all the wind turbines shall be designed for an ambient air temperature of – 20 °C to +50°C with a mean value +15°C such that operation shall be possible at ambient temperatures from –10°C to +40°C.

The above stress-strain data are then used to implement the Drucker-Prager values for our matrix material. The influence of temperature on other constituent materials is considered negligible. Hence after performing numerical analysis for different temperature data of epoxy, the results obtained suggest that while there is no significant effect of temperature on tensile strength, the elastic modulus decrease with increasing temperatures.

Modulus of elasticity values obtained at temperatures of -40° , 25° , 40° Celsius is 1810, 1316, 1060 Mpa respectively.

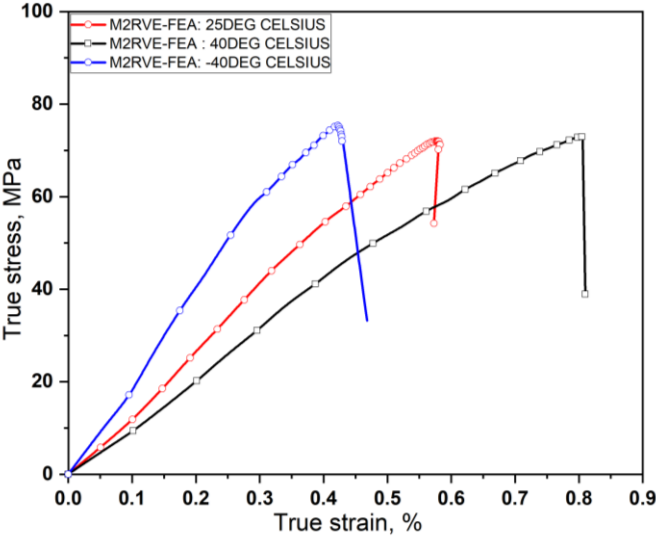


Fig.18. Stress strain response of M²RVE at different temperatures under transverse tension

4.2 Influence of Temperature on M²RVE under Transverse Compression:

To investigate the effect of temperature on M²RVE under Transverse Compression, epoxy E862 resin is considered. This type of resin is currently being used in aircraft engines. The experimental data available of this epoxy under compression are then used to provide the matrix material property data needed for analysis of M²RVE at different Temperatures. The experimental data provides the stress-strain behavior of matrix from room temperature of 25° Celsius to 80° Celsius.

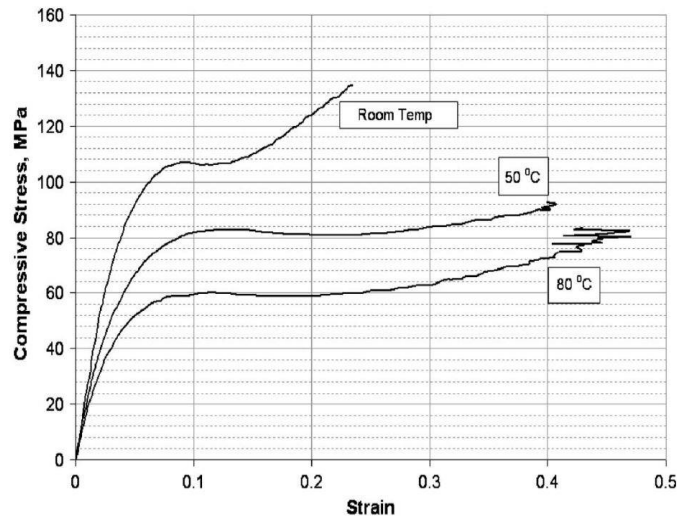


Fig.19. Stress strain response of epoxy E862 at different temperatures under transverse compression [21]

The compressive curves tended to rise after the yielding point because the original undeformed area increases as the specimen is loaded in compression.

Implementing this experimental data into the matrix material behavior, Numerical analysis is performed for different temperatures on M²RVE. The results suggest that with an increase in temperature both the modulus of elasticity and ultimate compressive strength decreases.

Modulus of elasticity at 25⁰, 50⁰,80⁰ Celsius are 1260, 1094, 991 Mpa.

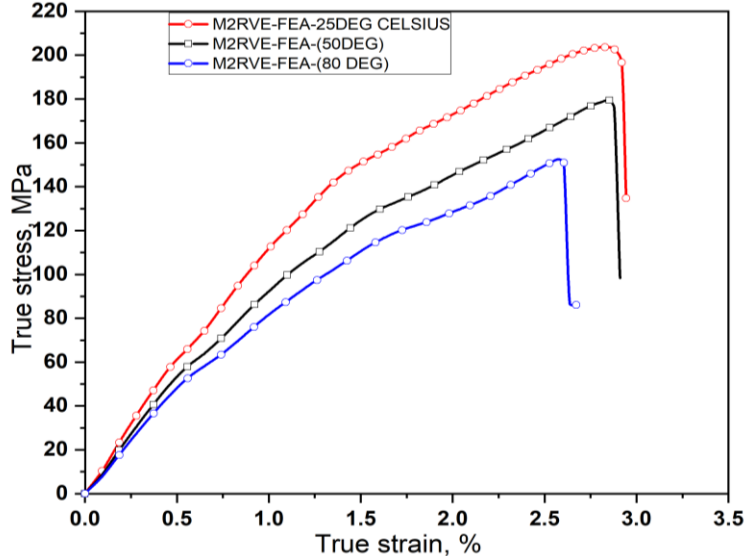


Fig.20. Stress strain response of M² RVE at different temperatures under transverse compression

4.3 Failure behavior of an epoxy resin under Transverse tension:

4.3.1 Introduction:

We observe from our studies that, the strength of glass-fiber reinforced composites is different under tension, compression and shear loading. It is mainly due to the fact that damage initiation and progression occurs differently in each of them. Hence, to describe and explain the role of the matrix in composites, the study of matrix properties is needed. When the composite is under various kinds of static loading (tension, compression, and shear loading), a tri-axial stress state occurs in the matrix. The failure of the composite is influenced by interface damage and matrix plasticity. It is often observed that, while the plain resin shows a rather brittle fracture behavior at a very low tensile strain, it yields and shows considerable plastic deformation in uni-axial compression or in pure shear. Even composites containing such brittle matrices can exhibit considerable plastic deformation at the micro-scale level. The strength of the composite also depends on the dimension of the test coupon.

4.3.2 Material and mechanical tests:

The Epoxy material and the hardner under consideration are HML-HinPoxy C Saturant and BHOR-Bhorbond EPCH hardner. It is a common epoxy resin from Hindustan composite solutions. Epoxy and hardner are mixed in the ratio 100:30 and stirred vigorously for (5-10) minutes. It is cured as slabs at 298 K for 48hr. The plain resin specimens were machined from the slabs of the resin. 5 Dog bone tensile specimens were prepared from the slab. The surfaces of the specimens were polished to decrease surface effects on mechanical properties. The dimensions of the cut specimens are according to **ASTM D638** is shown in the figure. The prepared specimen is then experimentally tested in a universal testing machine (UTM) and for all the tests crosshead speed is maintained at 1mm/min.

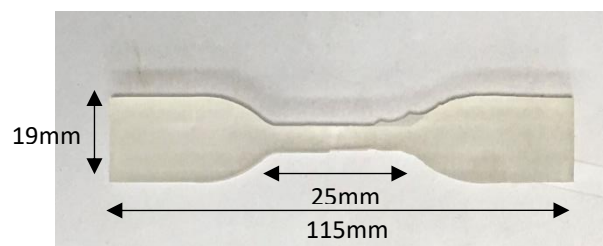


Fig 21: Tensile specimen[ASTM D638]

4.3.3 Results and discussion:

By definition, the linear part of the stress-strain behavior is taken as 0.05% nonlinear strain. True-stress and strain were considered as the obtained strains are very high and even change in the geometrical shape of the specimens is considerably high. The result of the tensile test is shown in the figure. In the beginning, stress increases linearly with the strain, it then follows a nonlinear deformation region and fractures. All the specimens show the same behavior and modulus obtained is 1.7Gpa and the ultimate tensile strength obtained is 63.81 Mpa.

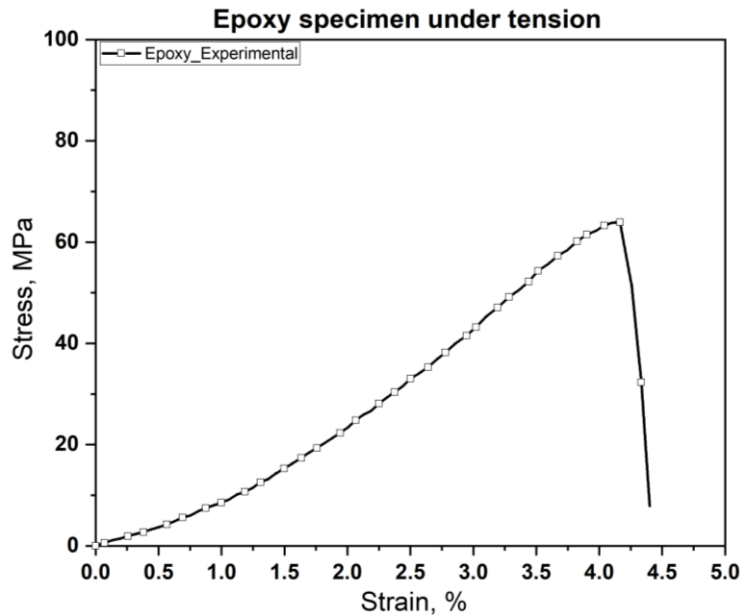


Fig 22: Stress-strain response of epoxy under

4.3.4 Conclusions:

The type of failure is brittle. The failure strains under tension is quite high. It is observed that there is matrix plasticity and it will lead to deformation rather than fracture. The large plastic deformation of the epoxy resin still has less influence on the final failure stress and the type of fracture is still brittle. The normal tensile stress controls crack propagation and the state of stress controls the plastic flow.



Fig 23:Specimen after failure

References

- [1] F. Naya, C. González, C. S. Lopes, S. Van der Veen, and F. Pons, “Computational micromechanics of the transverse and shear behavior of unidirectional fiber reinforced polymers including environmental effects,” *Compos. Part A Appl. Sci. Manuf.*, vol.92, no. January 2018, pp. 146–157, 2017.
- [2] J. Zangenberg, P. Brøndsted, and J. W. Gillespie, “Fatigue damage propagation in unidirectional glass fiber reinforced composites made of a non-crimp fabric,” *J.Compos. Mater.*, vol. 48, no.22, pp. 2711–2727, 2014.
- [3] M. A. Minnicino and M. H. Santare, “Modeling the progressive damage of the microdroplet test using contact surfaces with cohesive behavior,” *Compos. Sci.Technol.*, vol.72, no. 16, pp. 2024–2031, 2012.
- [4] L. Riaño, L. Belec, J. Chailan, and Y. Joli, “Effect of interphase region on the elastic behavior of unidirectional glass- fiber / epoxy composites,” vol. 198, no.Novembe 2017, pp. 109–116, 2018.
- [5] S. Sockalingam, M. Dey, J. W. Gillespie, and M. Keefe, “Finite element analysis of the microdroplet test method using cohesive zone model of the fiber / matrix interface,” *Compos. Part A*, vol. 56, pp. 239–247, 2014.
- [6] S. Tamrakar, Q. An, E. T. Thostenson, A. N. Rider, B. Z. G. Haque, and J. W. Gillespie, “Tailoring Interfacial Properties by Controlling Carbon Nanotube Coating Thickness on Glass Fibers Using Electrophoretic Deposition,” 2016
- [7] A. S. Kaddour and M. J. Hinton, “Input data for test cases used in benchmarking triaxial failure theories of composites,” *J. Compos. Mater.*, vol. 46, no. 19–20, pp. 2295–2312.
- [8] S. Daggumati, A. Sharma, and Y. S. Pydi, “Micromechanical FE Analysis of SiCf/SiC Composite with BN Interface,” *Silicon*
- [9] D. Garoz *et al.*, “Consistent application of periodic boundary conditions in implicit and explicit finite element simulations of damage in composites,” *Compos. Part B*, vol. 168, December 2018, pp. 254–266, 2019.
- [10] M. L. Benzeggagh and M. Kenane, “Measurement of Mixed-Mode Delamination Fracture Toughness of Unidirectional Glass /Epoxy Composites With Mixed-Mode Bending Apparatus,” vol. 56, pp. 439–449, 1996.
- [11] “ABAQUS (2010) Analysis User’s Manual. Version 6.10,” *Dassault Systemes Simulia, Inc.*
- [12] S. Sand-, J. F. Mandell, D. D. Samborsky, D. A. Miller, P. Agastra, and A. T. Sears, “SANDIA REPORT Analysis of SNL / MSU / DOE Fatigue Database Trends for Wind Turbine Blade Materials , 2010-2015,”.
- [13] Lei Yang¹ , Zhanjun Wu¹ , Yu Cao² and Ying Yan³ Micromechanical modelling and simulation of unidirectional fiber-reinforced composite under shear loading.

- [14] Mohammad A Torabizadeh Tensile , Compressive and Shear Properties of unidirectional glass/epoxy composites subjected to mechanical loading and low temperatureservices
- [15] John F. Mandell , Daniel D. Samborsky, and David A. Miller , Pancasatya Agastra and Aaron T. Sears Analysis of SNL/MSU/DOE Fatigue Database Trends for Wind Turbine Blade Materials, 2010-2015
- [16] Leon Mishnaevsky Jr. *, Povl Brøndsted Micromechanisms of damage in unidirectional fiber reinforced composites: 3D computational analysis
- [17] Leon Mishnaevsky Jr. *, Povl Brøndsted Micromechanical modeling of damage and fracture of unidirectional fiber reinforced composites: A review
- [18] Bodo Fiedler, Thomas Hobbiebrunken, Masaki Hojo, Karl Schulte, Influence of stress state and temperature on the strength of epoxy resins
- [19] E. Totry, C. González, and J. LLorca, “Failure locus of fiber-reinforced composites under transverse compression and out-of-plane shear,” *Compos. Sci. Technol.*, vol. 68, no. 3–4, pp. 829–839, 2008
- [19] C. González and J. LLorca, “Mechanical behavior of unidirectional fiber-reinforced polymers under transverse compression:Microscopic mechanisms and modeling,” *Compos. Sci. Technol.*, vol. 67, no. 13, pp. 2795–2806, 2007.
- [20] G. Catalanotti , P.P. Camanho, A.T. Marques Three-dimensional failure criteria for fiber-reinforced laminates
- [21] Justin D. Littell; Charles R. Ruggeri; Robert K. Goldberg; Gary D. Roberts; William A. Arnold; and Wieslaw K. Binienda Abstract: Measurement of Epoxy Resin Tension, Compression, and Shear Stress–Strain Curves over a Wide Range of Strain Rates Using Small Test Specimens
- [22] Vaidya RS, Sun CT. Prediction of composite properties from a representative volume element. *Composites Science and Technology*,56, pp.171–179 (1996).
- [23] Totry E, González C, LLorca J. Molina-Aldareguía J. Mechanisms of shear deformation in fiber-reinforced polymers: experiments and simulations. *International Journal of Fracture*,158, pp.197–209 (2009).
- [24] Soni, G, Singh, R, Mitra, M & Falzon, B 2012, 'A multi-fiber multi-layer representative volume element (M2RVE) for prediction of matrix and interfacial damage in composite laminates'
- [25] L. Yang, Y. Yan, Y. Liu, and Z. Ran, “Microscopic failure mechanisms of fiber-reinforced polymer composites under transverse tension and compression,”*Compos. Sci. Technol.*, vol. 72, no. 15, pp. 1818–1825, 2012